MATERIAL CONSIDERATIONS FOR TIME - DOMAIN OPTICAL STORAGE

Diploma paper by
Per Tidlund
LRAP - 131
Lund, June 1992

1. Introduction

The need for high density memories is to increase in a near future, due to that even the non specialist uses more advanced computers and computer applications. Today the utilisation of light seems to be the most promising way to achieve both high density storage and high speed processing. Light produced by a laser which can provide an extremely narrow linewidth, offers the possibilities of addressing individual energy levels in atoms and molecules. Of course if it would be possible to create a memory where, for instance, each excited atom correspond to a binary "1" and each ground state atom a "0", the "ultimate" memory would be born - reading and writing at the speed of light and offering a storage density of 10^{23} bits per cm^3. The storage capacity that the stimulated photon echo storage concept provides can't compete with the "ultimate" memory, but is a step in the right direction. The first steps toward storing data using stimulated photon echo in rare earth doped crystals were taken in 1987 by Ravinder Kachru et al. at SRI, California and at present a couple of hundred bits has been stored for some hours [13]. In this Diploma paper I show that, for the conventional approach to photon echo storage with destructive reading a theoretical analysis gives that for optically thin media the improvement in storage density that can be obtained by echo storage is marginal if any. With non-destructive reading the increase in storage density theoretically may increase to 250 times the theoretical limit of conventional optical storage. The performance of photon echo storage could change for optically dense samples. A definite statement of photon echo storage therefore have to wait until an analysis for optically dense media is performed.

2. Theory of the Photon Echo

We start this chapter with an explanation of the of the ordinary photon echo, section (2.1) and then extend it to the stimulated photon echo in section (2.2). The explanation given, is not the strict mathematical treatment, but rather one that gives a simple way of understanding what's happening. A more rigorous approach can be found in [1, 2]. Our treatment of the ordinary photon echo in (2.1) closely follows that by Durrant et al. [3].

2.1 The Photon Echo

Since the photon echo process is complex and involves a significant amount of quantum mechanics, we start with outlining the physical characteristic of the photon echo process and picture an analogy that helps us to get a grasp of the key element of the photon echo process. We aren't to begin with considering the general case of photon echo's generated by a sequence of many optical pulses, but only the case of a sequence of two optical pulses. Figure 1 illustrates the excitation pulse sequence and echo formation time in this case.

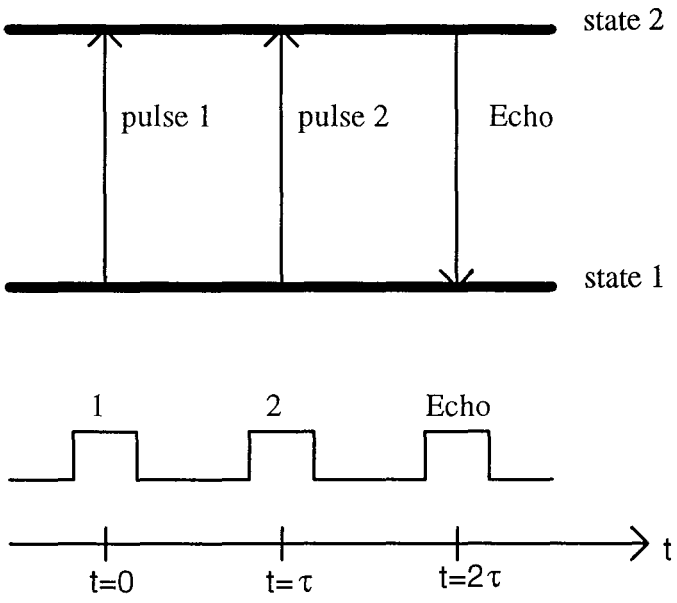

Fig. 1. Echo formation by excitation with two pulses. The sample is excited by a sequence of two short co - linear optical pulses tuned to resonance with a transition of energy hv. For pulses arriving at time's t = 0 and t = τ. the echo is emitted at time t = 2τ and co - propagate with the input pulse sequence.

Physical Characteristic of the Photon Echo Process:

Consider a system of two-level atoms. When resonant light interacts with this system the occupation number of the upper state increases. The atom is thus to be found more and more frequently in the upper state, while the occupation of the lower state decreases correspondingly. Eventually a state is reached in which the occupation numbers are equal. If one applies the external electric field to the atom for twice as long, it goes completely into the upper state. We now imagine that an atom has been excited to its upper state. It can be shown that the dipole moment of the atom then oscillates freely with the frequency of the optical transition, ω. According to Maxwell's theory, however, an oscillating dipole emits electro-magnetic waves, in this case light waves. This means that the ensemble of excited atoms emits light after the excitation. However, since the atoms are subject to different fields within the crystal, their transition frequencies are not all the same, and light emitted by oscillating dipoles with different frequencies will soon have different phases. The emitted intensity is therefore reduced. The key feature of the photon echo process is that a second pulse can bring the diverging phases of the oscillating dipoles back together in phase. As the oscillating dipoles come back into phase, they emit a light pulse which can be seen as the "Echo" of the previously applied pulses.

Analogy to the Photon Echo Process:

What happens can be compared with runners on a track. At the beginning of the race, all the runners are at the same place, the starting line. After the starting shot (write pulse), they have, however moved different distances away from the starting line because of their different running speed. If we think of a second gun shot as a signal for the runners to turn around and return to the start at the same speed as before. Obviously they all reach the start at the same time.

In the above description the runners symbolise the phase of the individual atomic dipoles and the gun shots corresponds to the excitation pulses.

2.1.1. The Response of an Atom to a Pulse of Resonant Light

Consider the response, when a pulse of resonant light interacts with a single atom. This atom is completely isolated from the influences of other atoms. The Schrödinger equation for the interaction of a two-level atom with a coherent radiation field, has the form

$$\left(\mathbf{H}+\mathbf{H}^{*}\right)\Psi(\vec{r},t)=i\hbar\frac{d}{dt}(\Psi(\vec{r},t)) \tag{2.1}$$

if we neglect homogeneous decay effects. Here H is the Hamiltonian for an electron moving in the potential field V of the nucleus. H^* is the radiation dependent part of the Schrödinger equation. We are from here on using a somewhat different notation (Ket notation), that is

$$\Psi(\vec{r},t)=|\vec{r},t\rangle \tag{2.2}$$

We assume that we already solved the Hamiltonian equation

$$\mathbf{H}|\vec{r}\rangle=E_i|\vec{r}\rangle \qquad \text{i=1,2} \tag{2.3}$$

where E_i is the energy. To find the explicit form of H^*, let us picture the radiation field as a plane wave:

$$\vec{E}=\vec{E}_0\cos(\vec{k}\cdot\vec{r}-\omega t) \tag{2.4}$$

Then the interaction with a laser pulse, in the electric dipole approximation, can be taken to be

$$\mathbf{H}^{*}=-\vec{E}(\vec{r},t)\mathbf{d} \tag{2.5}$$

We assume, furthermore, that the atom is localised at position **r**. With the simple two-state model, a general state of the atom at any time t can be represented by the ket

$$|\vec{r},t\rangle=c(t)|1\rangle+d(t)e^{-i\Omega t}|2\rangle=\begin{pmatrix} c(t) \\ d(t)e^{-i\Omega t}\end{pmatrix} \tag{2.6}$$

where the kets represents the two orthonormal eigenstates of the atomic Hamiltonian with eigenvalues 0 and $(h/2\pi)\omega$, and c(t) and $d(t)\exp(-i\Omega t)$ are the time-dependent amplitudes in the Schrödinger representation. The factor $\exp(-i\Omega t)$ represent the free evolution of the atom under action of the unperturbed Hamiltonian.

The radiation dependent part of the Hamiltonian is

$$\mathbf{H}^* = \cos(\omega t - \vec{k}\cdot\vec{r})\mathbf{h}^* = \begin{pmatrix} 0 & -E_0\cos(\omega t - \vec{k}\cdot\vec{r})d_{dipol} \\ -E_0\cos(\omega t - \vec{k}\cdot\vec{r})d_{dipol} & 0 \end{pmatrix} \quad (2.7)$$

where I have introduced the abbreviation

$$\mathbf{h}^* = -\vec{E}_0\mathbf{d} = \begin{pmatrix} 0 & -E_0 d_{dipol} \\ -E_0 d_{dipol} & 0 \end{pmatrix} \quad (2.8)$$

We have in equation (2.8) used that for electric dipole transitions it is reasonable to assume that the diagonal elements of H* vanish, due to symmetries and selection rules. In order to determine the still unknown coefficients c(t) and d(t), we calculate the expectation value of the Schrödinger equation, Eq. (2.1).

$$\langle s|\mathbf{H} + \mathbf{H}^*|\vec{r},t\rangle = \langle s|i\hbar\frac{d}{dt}|\vec{r},t\rangle \quad (2.9)$$

for $\langle s| = \langle 1|$ and $\langle 2|$. This yields

$$\mathbf{H}_{11}c(t) + \mathbf{H}_{12}^* d(t)e^{-i\Omega t} = i\hbar\frac{d}{dt}c(t) \quad (2.10)$$

$$\mathbf{H}_{21}^* c(t) + \mathbf{H}_{22}d(t)e^{-i\Omega t} = i\hbar\frac{d}{dt}\left[d(t)e^{-i\Omega t}\right] \quad (2.11)$$

If we rearrange slightly, we obtain

$$\mathbf{H}_{11}c(t) + \mathbf{H}_{12}^* d(t)e^{-i\Omega t} - i\hbar\frac{d}{dt}(c(t)) = 0 \quad (2.12)$$

$$\mathbf{H}_{21}^* c(t) + \left[\mathbf{H}_{22} - \hbar\Omega\right]d(t)e^{-i\Omega t} - i\hbar\frac{d}{dt}(d(t))e^{-i\Omega t} = 0 \quad (2.13)$$

From these equations we obtain the resulting equations for the time-dependent amplitudes in the Schrödinger representation:

$$\frac{d}{dt}c = -id(t)\frac{\mathbf{h}_{12}^*}{2\hbar}\left[e^{i((\omega-\Omega)t-\vec{k}\vec{r})} + e^{-i((\omega+\Omega)t-\vec{k}\vec{r})}\right] \quad (2.14)$$

$$\frac{d}{dt}d = -ic(t)\frac{\mathbf{h}_{21}^{*}}{2\hbar}\left[e^{-i((\omega-\Omega)t-\vec{k}\vec{r})}+e^{i((\omega+\Omega)t-\vec{k}\vec{r})}\right]+i(\Omega-\omega)d(t) \tag{2.15}$$

If we in equation (2.13) use the fact that the value of the ordinary Hamiltonian components $\mathbf{H}_{11}$ and $\mathbf{H}_{22}$ equals 0 and $(h/2\pi)\omega$ and the abbreviation introduced in (2.7), then is it straightforward to obtain equation (2.14) from (2.12) and equation (2.15) from (2.13).

2.1.2. The Rotating Wave Approximation

The "rotating wave approximation" means, that the "non-resonant" term oscillating at frequency $\omega+\Omega$ is neglected. That this approximation is valid, can be realized in the following way; c(t) and d(t) vary quite slowly in time compared to the frequency $\omega+\Omega$. This makes it possible for use to average (2.14) and (2.15) over a time which is large compared to $1/(\omega+\Omega)$, but still short compared to the time constant that determines the change in c(t) and d(t). The result of this averaging is that the rapidly changing term $\omega+\Omega$ makes negligible contribution. We now introduce the further assumption that the field is in resonance with the electronic transition ($\omega=\Omega$). This gives the following equations

$$\frac{d}{dt}c = -id(t)\frac{\mathbf{h}_{12}^{*}}{2\hbar}e^{-i\vec{k}\vec{r}} \tag{2.16}$$

$$\frac{d}{dt}d = -ic(t)\frac{\mathbf{h}_{21}^{*}}{2\hbar}e^{i\vec{k}\vec{r}} \tag{2.17}$$

To solve these equations, we first take the time derivative of (2.16):

$$\frac{d^2}{dt^2}(c(t)) = -i\frac{d}{dt}(d(t))\frac{\mathbf{h}_{12}^{*}}{2\hbar}e^{-i\vec{k}\vec{r}} \tag{2.18}$$

and then, substitute (2.17). This yields

$$\frac{d^2}{dt^2}(c(t))+c(t)\frac{\mathbf{h}_{21}^{*}\mathbf{h}_{12}^{*}}{4\hbar^2} = 0 \tag{2.19}$$

We recognise (2.19) as a typical oscillator equation with the general solution

$$c(t) = C_1 \sin\left(\sqrt{\frac{\mathbf{h}_{21}^{*}\mathbf{h}_{12}^{*}}{4\hbar^2}}t\right) + C_2 \cos\left(\sqrt{\frac{\mathbf{h}_{21}^{*}\mathbf{h}_{12}^{*}}{4\hbar^2}}t\right) \tag{2.20}$$

Using (2.16) and (2.20) we obtain

$$d(t) = D_1 \sin\left(\sqrt{\frac{\mathbf{h}_{21}^{*}\mathbf{h}_{12}^{*}}{4\hbar^2}}t\right) + D_2 \cos\left(\sqrt{\frac{\mathbf{h}_{21}^{*}\mathbf{h}_{12}^{*}}{4\hbar^2}}t\right) \tag{2.21}$$

where the amplitudes are free to vary. If one substitute these equation's in (2.16), (2.17) and integrate with the use of that we know the initial amplitude's $c(t_1)$ and $d(t_1)$, one gets the following solutions for a pulse of length t_p:

$$c(t_1+t_p)=Ac(t_1)+iBe^{(-i\vec{k}\cdot\vec{r})}d(t_1) \tag{2.22}$$

$$d(t_1+t_p)=iBe^{(i\vec{k}\cdot\vec{r})}c(t_1)+Ad(t_1) \tag{2.23}$$

where $A\equiv\cos(\theta/2)$ and $B\equiv\sin(\theta/2)$ and θ is the pulse area and equals

$$\theta \equiv \frac{\sqrt{\mathbf{h}_{21}^{*}\mathbf{h}_{12}^{*}}t_p}{\hbar} \tag{2.24}$$

To get a picture of what happens when a laser pulse with pulse area θ and propagation vector **k** interacts with the atom, I use the atomic state amplitude evolution diagram shown in figure 2. This shows that when the laser light interacts with the sample, represented by the two-state atomic model, then time-dependent amplitudes of the two states are mixed. As we will see later it is the state amplitudes mixing that are the key to the creation of the photon echo. What is most important to notice in the diagram is that the atomic amplitude multiplied by a factor corresponding to the strength of the optical pulse is transferred between the two atomic states.

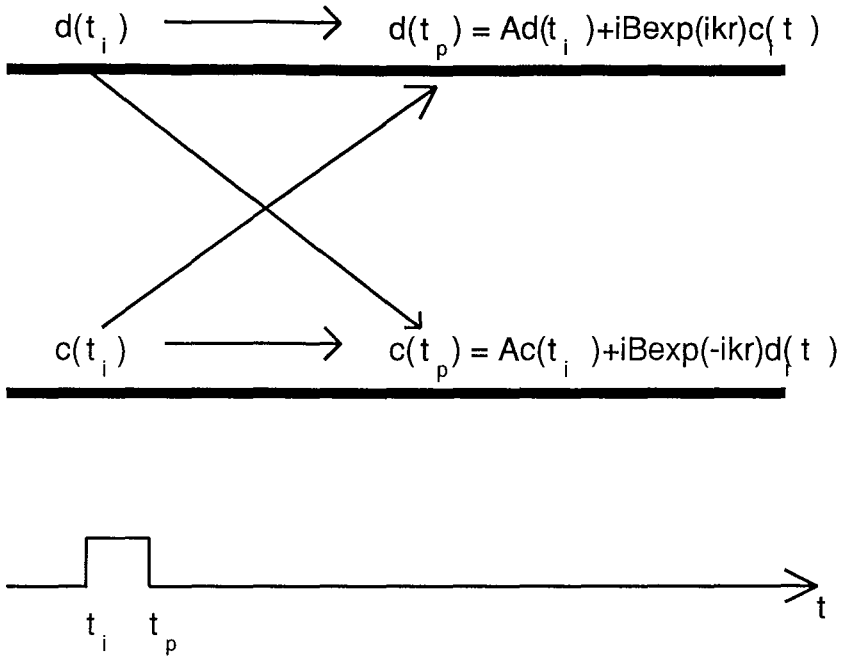

Fig. 2. Time evolution diagram of the atomic state amplitude from equation's (2.22) and (2.23). The picture shows a two-state atom under the influence of a resonant optical pulse of pulse area θ and propagation vector **k**. The arrows between the states indicate upwards and downwards transitions where amplitude is transferred between the states. $A \equiv \cos(\theta/2)$ and $B \equiv \sin(\theta/2)$.

2.1.3. Time Dependence of the Sample Polarisation

In order to bee able to calculate the polarisation of the sample, have we first to obtain an expression for the dipole moment of a single atom. Then is it only to perform the summation of the atomic dipole moment over a volume of the sample. The polarisation is then obtained by simply dividing the sum with the volume.

Let us assume that the atom is initially in it's ground state corresponding to c(t=0)=1 and d(t=0)=0. Then the atomic dipole moment, D, induced by the pulse is

$$D(\vec{r},t_p)=\left\langle \vec{r},t_p\left|\mathbf{d}\right|\vec{r},t_p\right\rangle=\begin{pmatrix}c(t_p)^* & d(t_p)^* e^{i\Omega t}\end{pmatrix}\begin{pmatrix}0 & d_{dipol}\\ d_{dipol} & 0\end{pmatrix}\begin{pmatrix}c(t_p)\\ d(t_p)e^{-i\Omega t}\end{pmatrix}$$

$$=c(t_p)^* d(t_p)e^{-i\Omega t}d_{dipol}+C.C. \tag{2.25}$$

where C.C. is the complex conjugate. If we use the result that we obtained in equation (2.22) and (2.23) with $t_1 = 0$, then can we rewrite the atomic dipole moment as

$$D(\vec{r},t_p)=\frac{1}{2}id_{dipol}(t_p)\sin(\theta)e^{i\vec{k}\cdot\vec{r}}+C.C. \tag{2.26}$$

where $d_{dipol}(t) \equiv e^{-i\Omega t}d_{dipol}$ have been introduced for convenience.

Now, consider a sample consisting of N atoms, which all are excited with the same amplitude and with the same phase by a plane wave with propagation vector **k**. Then immediately after the pulse, we have a total polarisation of $N \cdot D(\mathbf{r},tp)$. If we assume that the inhomogeneous broadening of the transition frequency can be described by a normalized distribution function $\rho(\Delta)$, where $\omega+\Delta$ is the transition resonant frequency of an atom in the sample. Then if we have an atom with resonant frequency $\omega+\Delta$ the atomic amplitude evolution diagram looks like that in figure 3.

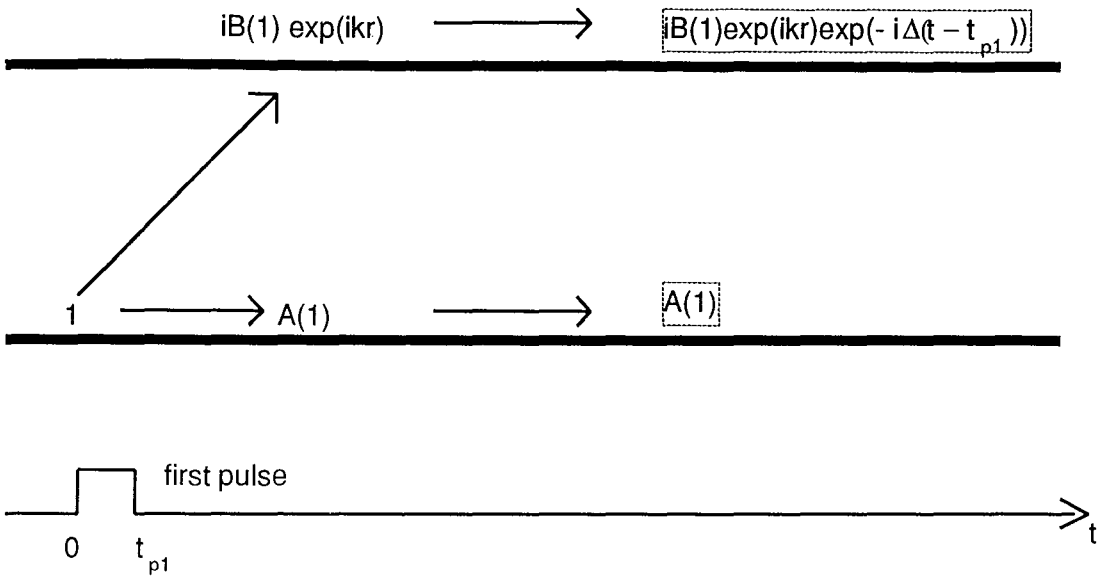

Fig. 3. Atomic amplitude evolution diagram for pulsed excitation and subsequent free evolution of an atom of resonance frequency $\omega + \Delta$ initially in the ground state in a inhomogeneously broadened sample. The upper state has a time - dependent phase factor. This gives a time-dependent dipole moment. The dipole moment of the system is calculated from equation (2.26) using the terms in the boxes above. A(1) = $\cos(\theta 1/2)$ and B(1) = $\sin(\theta 1/2)$ where $\theta 1$ pulse area for the first pulse.

We see from the term $\exp(-i\Delta(t - t_{p1}))$ in figure 3 that atoms in the sample with different transition frequencies, caused by the inhomogeneous broadening, have different phase relations at a time $t > t_{p1}$. If we now calculate the atomic dipole moment then we get

$$D(\vec{r},t) = \langle \vec{r},t|\mathbf{d}|\vec{r},t\rangle = \begin{pmatrix} A(1) & -iB(1)e^{-i\vec{k}\cdot\vec{r}}e^{i\Delta(t-t_{p1})} \end{pmatrix} \begin{pmatrix} 0 & d_{dipol} \\ d_{dipol} & 0 \end{pmatrix} \begin{pmatrix} A(1) \\ iB(1)e^{i\vec{k}\cdot\vec{r}}e^{-i\Delta(t-t_{p1})} \end{pmatrix}$$

$$= \frac{1}{2} i d_{dipol}(t)\sin(\theta) e^{i(\vec{k}\cdot\vec{r}-\Delta(t-t_p))} + CC. \qquad (2.27)$$

Polarization of a sample is the contribution from all the atomic dipole moments in a sample per unit volume to a specific point **r**. If the sample contains N contributing parts per cubic meter that oscillate with different frequency. Then it is straightforward to calculate polarization through a simple integration over all the frequency components in the volume of interest.

The polarisation of the sample P(**r**,t), at a position **r** and at time t > tp:

$$P(\vec{r},t)=\frac{i}{2}Nd_{dipol}(t)\sin(\theta)e^{i(\vec{k}\cdot\vec{r})}\int_{-\infty}^{+\infty}\rho(\Delta)e^{-i\Delta(t-tp)}d\Delta+C.C. \tag{2.28}$$

where ρ(Δ) describe the relative number of active atoms that have a frequency between ω and ω + Δ.

One can from (2.28) see that the polarization of the sample is a decreasing function with time. The relation between emitted intensity and the sample polarization is

$$I\propto|P(\vec{r},t)|^2 \tag{2.29}$$

this means that the light emitted by the sample is a decreasing function of time.

2.1.4. Echo formation

We now let a second pulse interact with the sample, from figure 4 it is seen that the ground state term is phase advanced with respect to an upper state term.

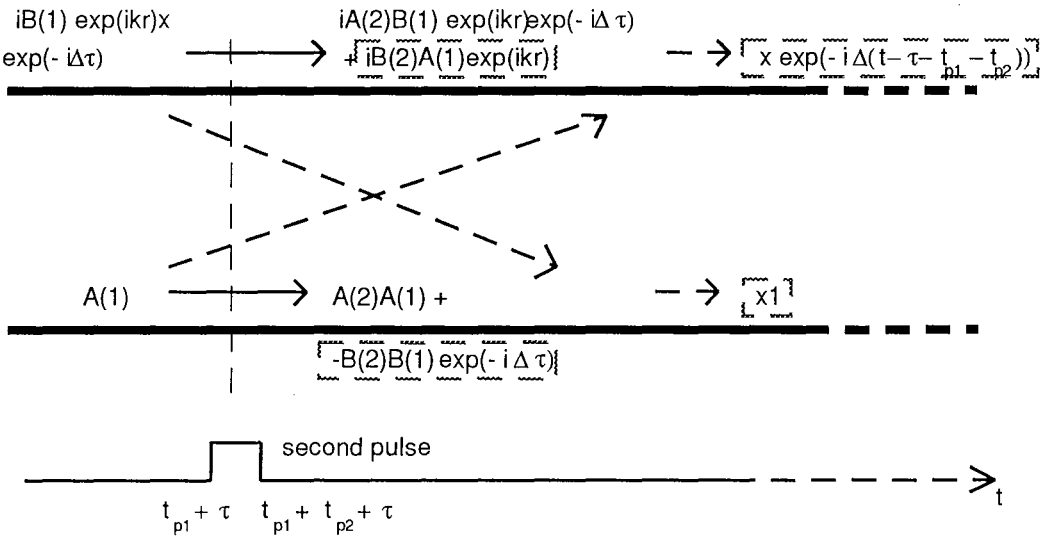

Fig. 4. Atomic amplitude evolution diagram for the second pulse and subsequent free evolution of an atom of resonance frequency ω + Δ. When an expression begins with X, it means that it has to be multiplied by the earlier expression. The upper and lower state amplitudes are coupled through equation (2.27) and the expressions inside the boxes are responsible for the echo generation. A(2) = cos(θ2/2) and B(2) = sin(θ2/2).

At a time τ after the second pulse there is no phase difference between the upper and lower state, then the polarisation in the sample has passed a second maximum. The time-dependence of the atomic dipole moment after the second pulse has interacted with sample is calculated from the terms inside the boxes in figure 4.

$$D(\mathbf{r},t)=\langle\vec{r},t|\mathbf{d}|\vec{r},t\rangle=\begin{pmatrix}-B(2)B(1)e^{i\Delta\tau} & -iB(2)A(1)e^{-i\vec{k}\cdot\vec{r}}e^{i\Delta(t-\tau-t_{p1}-t_{p2})}\end{pmatrix}$$

$$\begin{pmatrix}0 & d_{dipol}\\ d_{dipol} & 0\end{pmatrix}\begin{pmatrix}-B(2)B(1)e^{-i\Delta\tau}\\ iB(2)A(1)e^{i\vec{k}\cdot\vec{r}}e^{i\Delta(t-\tau-t_{p1}-t_{p2})}\end{pmatrix}=$$

$$-\frac{i}{2}d_{dipol}(t)\sin(\theta_1)\sin(\frac{\theta_2}{2})^2 e^{i\left[\vec{k}\cdot\vec{r}-\Delta(t-2\tau-t_{p1}-t_{p2})\right]}+CC. \tag{2.30}$$

And the corresponding polarisation is obtained in the same way as in the preceding section.

$$P(\vec{r},t)=-\frac{1}{2}iNd_{dipol}(t)\sin(\theta_1)\sin(\frac{\theta_2}{2})^2 e^{i(\vec{k}\cdot\vec{r})}$$
$$x\int_{-\infty}^{+\infty}\rho(\Delta)e^{-i\Delta(t-2\tau-t_{p1}-t_{p2})}+CC. \tag{2.31}$$

If we assume that distribution function, ρ(Δ), can be approximated by a gaussian function, then can we evaluate the integral. The peak intensity of the echo is (assuming tp1, tp2 << τ)

$$I_{peak}\propto|P(\vec{r},2\tau)|^2=\frac{1}{4}N^2\sin(\theta_1)^2\sin(\frac{\theta_2}{2})^4 \tag{2.32}$$

The echo's intensity depends on the density of active centers, pulse area of the first and second laser pulse, but from (2.31) we see that the time when the echo is formed depends only on the time τ between the two pulses. Results can easily be generalized to a system of more than two pulses and with pulses that aren't co-linear here we just give the results.

2.1.5. Multiple Data Pulses and Non Co-linear Excitation Pulses

Multiple data pulse echo formation can be represented in the following way, θ_1 is the first pulse (write pulse), θ_i is the i:th data pulse in a sequence of pulses that correspond to the data that are to be stored and θ_3 is the read pulse that forces the echo to emerge. The echo corresponding to the i:th data pulse, then has the form:

$$I_i \propto |P(\vec{r},2\tau)|^2 \propto N^2 \sin(\theta_1)^2 \sin(\theta_i)^2 \sin(\theta_3)^2 \tag{2.33}$$

I have in equation (2.33) again assumed that we can neglect the pulse interaction time in comparison with the pulse duration. If the write pulse and the data pulse sequence propagates at a small angle ϕ from the read pulse the echo is emitted in a direction 2ϕ from the read pulse.

2.2. Stimulated Photon Echo

To understand how any information can be stored in a sample using the photon echo concept, we consider what happens to the population of atoms which at the beginning all are situated in the ground state [4].

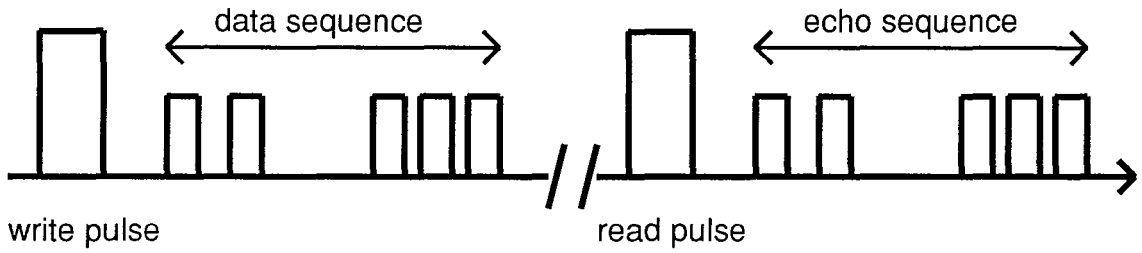

Fig. 5. Pulse sequence.

When the first pulse(write) interacts with the sample, the pulse produces a population distribution of atoms in the upper level. That is the laser pulse transfer some of the atoms to their excited state. If we look at the atoms in the sample all together, then can we picture that we have an excited state that can be thought of as a continuum of levels. In some of the levels in this continuum have we transferred atoms with the laser pulse(write pulse). This means that we have created a population distribution in the excited state of the sample. This population distribution starts immediately to relax due homogeneous and inhomogeneous relaxation processes.

Later, when the data pulse sequence at some time after the write pulse interact with the sample, the relaxed population distribution in the excited state will be modulated. This modulation is due to either constructive or destructive interference between the electromagnetic field of the data pulses and the dipoles created by the first pulse. The dipoles that are in phase with the second, which arrives at a time, τ, are all those with a detuning $\Delta\nu$ from the laser frequency ν_0 where the detuning, $\Delta\nu$, multiplied by the time between the pulses, τ, equals an integer. This results increased excitation of these atoms and a corresponding increase of the population in the excited state. If $\Delta\nu\cdot\tau$ on the other hand equals half of an integer, then the dipoles are out of phase with the second pulse and a decrease in the excited state population will be observed.

In the previous section it was shown that for the ordinary photon echo process the echo was emitted from the sample at a time completely decided by the time between the first and second pulse. This makes the photon echo process disadvantageous for storage of data, because when we have stored data, then we want to be able decide when to read the stored data, by sending an external signal to the sample. To understand how this can be

the readout process due to the fact, that in excitation out of a specific ground state hyperfine level nuclear spin reorientation may occur and we then does not know which excited state we are to end up in.

Excitation of the sample with a read pulse, figure 5, forces the modulated population distribution in the hyperfine structure of the ground level ($^3H_4$) to transfer to the hyperfine structure of the excited state. We now have an analogue to the case I describe in section (2.1.4) on Echo Formation. The sample radiates the stored data pulse and the time when this radiation accrues is completely decided by the read pulse. A fundamental difference between the photon echo and the stimulated photon echo process is that in the stimulated photon echo process we already have the information in the sample and only have to transfer it to the excited state any time we wish read it.

3. Material Considerations for Time-Domain Optical Storage

The need for optical storage of information is to increase in a near future, due to the increased use of optical - processing and computers. It is therefore important to know the allowed material parameter space for the possible storage methods. Our aim here is to decide this parameter space for the stimulated photon echo storage concept in optically thin media.

3.1. Model

The total number of photons in the stimulated photon echo is given by equation (3.1). This expression is a modified version of that given by Abella et al. [6], where branching ratio, write-,data- and read-pulse areas have been included.

$$\Pi=\frac{3}{32}\frac{\eta_q}{\sqrt{\varepsilon}}\lambda\eta^2 A_x{}^2 n^2 L T_{inh}{}^2 \frac{A}{\tau}\sin^2(\theta_W)\sin^2(\theta_D)\sin^2(\theta_R) \tag{3.1}$$

where

n = Density of storage centers
A_X = Laser focal spot area
L = Length of storage volume
A = Einstein coefficient for the transition
T_{inh}= Inhomogeneous relaxation time
τ = Duration of each data bit
η = Branching ratio for $\Delta m \neq 0$ hyperfine transitions
η_q = Quantum efficiency of detector
λ = Excitation wave length
ε = Index of refraction squared of sample material
θ_W, θ_D ,θ_R = Pulse areas for write, data and read pulses

(Henceforth $\eta_q = 0.75$, $\varepsilon = 3$, $\theta_W = \pi/2$ and $\theta_R = \pi/2$.) This expression is valid only for small Fresnel numbers, $A << 4L\lambda$, ([6], appendix C). To fulfil this condition, at least approximately, we select the length of the storage volume to twice the Rayleigh length ($L= 2A_X/\lambda$). Furthermore we have assumed that the direct optical transition branching ratio is much smaller than the total transition branching ratio (Appendix A), and that the branching ratio for direct optical transitions therefore can be neglected. In order to be able to compare the storage density of the photon echo method with the storage density obtain with ordinary optical storage methods, I introduce the parameter k in the following way $A = (k\lambda)^2$. The storage densities that we are able to achieve with ordinary optical storage methods are $1/\lambda^2$. Furthermore it is assumed that the number of stored data bits (N) within the laser focal volume is a large number. Assuming a data sequence of N bits such that $N\theta_D = \pi/2$ we can then write $\sin(\theta_D) \cong \pi/(2N)$.

With these conditions are we able to rewrite equation (3.1). This yields

$$\Pi=\frac{3\pi^2}{64}\frac{\eta_q}{\sqrt{\varepsilon}}n^2k^6\lambda^6\eta^2\frac{T_{inh}^2}{N^2}\frac{A}{\tau} \tag{3.2}$$

If we specify the number of photons (Π), we do that later on, then we are able to obtain an expression for the fractional increase in storage density (N/k^2) compared to the ordinary storage density of optical methods ($1/\lambda^2$) as a function of hyperfine branching ratio (η), concentration of ions (n), the Einstein coefficient for the transition (A), the pulse length for one data bit (τ) and the inhomogeneous relaxation time T_{inh}.

$$\frac{N}{k^2}=\frac{\pi}{8}\sqrt{\frac{3\eta_q}{\sqrt{\varepsilon}}}nk\lambda^3\eta\frac{T_{inh}}{\tau}\sqrt{\frac{A\tau}{\Pi}} \tag{3.3}$$

3.1.1. Limit set by the inhomogeneous relaxation time

We have to avoid excessive spectral diffusion[7]. This means that we can not allow the interaction between the doping ions to bee too severe. This then puts a limit on the maximum value of the density of storage centers, n, of about $n_{max}=10^{26}$ /m^3. It is clear from equation (3.3) that in order to obtain a large fractional increase in storage density (N/k^2) that we should choose the duration of each data bit (τ) as small as possible. The smallest possible value for the data bit duration is when it equals the value of the inhomogeneous relaxation time, $\tau = T_{inh}$.

With equation (3.3) and the fact that the data bit duration must be larger than or equal to the inhomogeneous relaxation time, $\tau > T_{inh}$, can we express an upper limit of the fractional increase in storage density as

$$\frac{N}{k^2}\le\frac{\pi}{8}\sqrt{\frac{3\eta_q}{\sqrt{\varepsilon}}}n\lambda^3k\eta\frac{1}{\sqrt{\Pi}}\sqrt{A\tau} \tag{3.4}$$

If we assume that the inhomogeneous line width can be approximated by an gaussian function, then can we express the inhomogeneous relaxation time, T_{inh}, as[8]

$$T_{inh}=4\sqrt{\frac{\pi}{\ln(2)}}\frac{1}{\lambda^2}\frac{\sigma}{A} \tag{3.5}$$

where σ is the peak absorption cross section. Equation (3.5) enables us to eliminate the inhomogeneous relaxation time, T_{inh}, dependence in the expression for the fractional increase in storage density, equation (3.3). This yields that the fractional increase in storage density (N/k^2) can be rewritten as

$$\frac{N}{k^2}=\frac{\pi}{4}\sqrt{\frac{3\pi\eta_q}{\ln(2)\sqrt{\varepsilon}}}(n\sigma L)\frac{\eta}{k}\frac{1}{\sqrt{\Pi}}\frac{1}{\sqrt{(A\tau)}} \tag{3.6}$$

3.1.2. Optically thin medium

As only optically thin media are considered, there is an upper limit on the absorption coefficient ($\alpha=n\sigma L$). This is, somewhat arbitrarily, chosen to $n\sigma L \leq 0.3$. The reason for restricting our analysis to optically thin media, is that for optically thick media we can not consider that the medium to be homogeneously excited by the laser pulses. This makes the analysis tremendously more complex. Now we can with this upper limit on the absorption coefficient and equation (3.6) again gets an upper limit on the fractional increase in storage density (N/k^2)

$$\frac{N}{k^2}\leq\frac{3\pi}{40}\sqrt{\frac{3\pi\eta_q}{\ln(2)\sqrt{\varepsilon}}}\frac{\eta}{k}\frac{1}{\sqrt{\Pi}}\frac{1}{\sqrt{(A\tau)}} \tag{3.7}$$

3.2. Noise Mechanism

We now need to make assumptions of how many photons that the echo necessary must contain in order to obtain a reasonable signal to noise. The noise mechanisms that are valid in our case are the spontaneous emission noise, scattered light and different noise mechanisms in the photomultiplier[9].

Spontaneous noise: The spontaneous noise is due to the spontaneous emission of light in the crystal under the time τ, this spontaneous emission is at least approximately the same in all directions and we have only to take into account that amount of light that are in the direction of the detector. An estimation of the number of spontaneous emitted photons under one second is

$$\frac{\Omega}{4\pi} n(A_x l) \frac{T_{inh}}{\tau} A \tag{3.8}$$

where Ω is space angle of the detector.

Scattered light: This light is primarily due to limited ability to switch off the excitation light when the photon echo is recorded by the detector.

Noise mechanisms in the photomultiplier: In the photomultiplier the noise is due to cathode shot noise, dynode shot noise and Johnson noise. Shot noise is caused by fluctuations in the electron current that are due to the discrete nature of the photons. Dynode shot noise is the shot noise due to the random nature of the secondary electron emission process at the dynodes. Since current originating at a dynode does not experience the full gain of the tube, the contribution of all the dynodes to the total shot noise output is smaller by a factor of δ^{-1} then that of the cathode(where δ is the dynode amplification factor); since $\delta \cong 5$ it amounts to small correction and will be ignored in the following. Johnson noise is due to the fluctuations in the voltage across a resistor. These fluctuations are often caused by thermal motion of the charge carriers.

The fundamental noise limit in our analysis is the **Cathode shot noise**, from here on referred to as **shot noise**. The shot noise is the square root of the number of photons in the echo, we can now express the **Signal to Noise Ratio (SNR)** in the following way

$$SNR = \frac{\Pi}{\sqrt{\Pi}} = \sqrt{\Pi} \tag{3.9}$$

We suppose that we need a signal-to-noise ratio, SNR, of the order of 10. A value of the signal-to-noise ratio of 10 corresponds to that we have to detect 100 photons at the detector to achieve the required SNR (e. g. [10]).

3.3. First Read

With the restrictions given by equations (3.4) and (3.7) together with the fact that we have chosen the number of required photons in the echo, Π, to equal 100 we are now able to present primarily allowed regions in (Aτ,η) space for any given value of the fractional increase in storage density , N/k^2

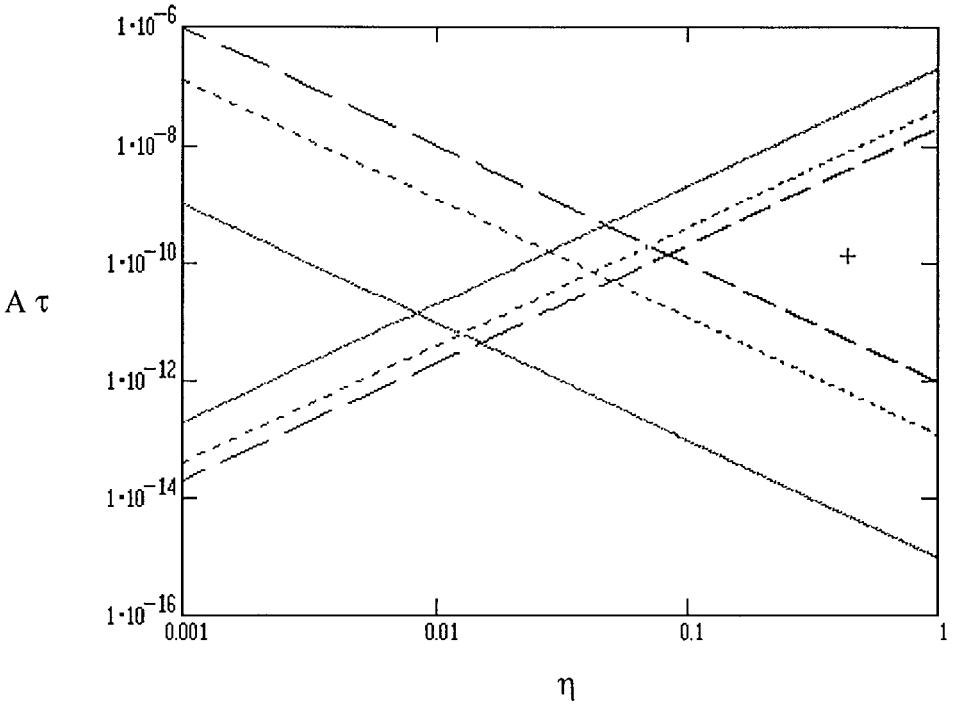

Fig. 7. The allowed region (marked with +) for the first read in η (hyperfine transition branching ratio) vs. Aτ (transition probability · data bit duration) space for a fractional increase in storage density of $N/k^2 = 2$ (limited by the solid lines), $N/k^2 = 10$ (limited by the dotted lines) and $N/k^2 = 20$ (limited by the dashed lines).

It is assumed that 1 kbyte (8·1024 bits) is stored in each single point. From figure 7 we see that the allowed region shrinks drastically when the fractional increase in storage density (N/k^2) increase. For a fractional increase in storage density of 2 are the allowed values of the branching ration $0.01 < \eta < 1$ and the allowed values of Einstein coefficient times the data bit duration $10^{-15} < A \cdot \tau < 10^{-7}$. If a fractional increase in storage density of 10 is required then the allowed parameter space shrinks to $0.1 < \eta < 1$ and $10^{-13} < A \cdot \tau < 10\text{-}8$. Furthermore, in the photon gating case, $\eta = 1$, the largest possible fractional increase in storage density, N/k^2, equals 250 at an $A \cdot \tau$ value of 10^{-8}.

3.4. Multiple Reads

To obtain expressions that are valid for multiple reads we have to consider what happens when the relaxed storage media interact with the second(read) pulse. In the medium the fraction (1-η) of the original information is again stored in the hyperfine structure after the first read pulse. When the read pulse interacts with the sample, the fraction (1-η0) of the information stored in the relaxed medium is transferred to an exited level, here η0 is the optical transition branching ratio and we can in comparison with the total branching ratio regard it as zero. For i reads then, we have to replace η with η(1- η)$^{i-1}$ in the previous equations to obtain the adequate expressions for multiple reads. It then follows from Equations (3.4) and (3.7) that

$$\frac{N}{k^2} \le \frac{\pi}{8}\sqrt{\frac{3\eta_q}{\sqrt{\varepsilon}}} n\lambda^3 k\eta(1-\eta)^{i-1}\frac{1}{\sqrt{\Pi}}\sqrt{A\tau} \tag{3.10}$$

$$\frac{N}{k^2} \le \frac{3\pi}{40}\sqrt{\frac{3\pi\eta_q}{\ln(2)\sqrt{\varepsilon}}}\frac{\eta(1-\eta)^{i-1}}{k}\frac{1}{\sqrt{\Pi}}\frac{1}{\sqrt{(A\tau)}} \tag{3.11}$$

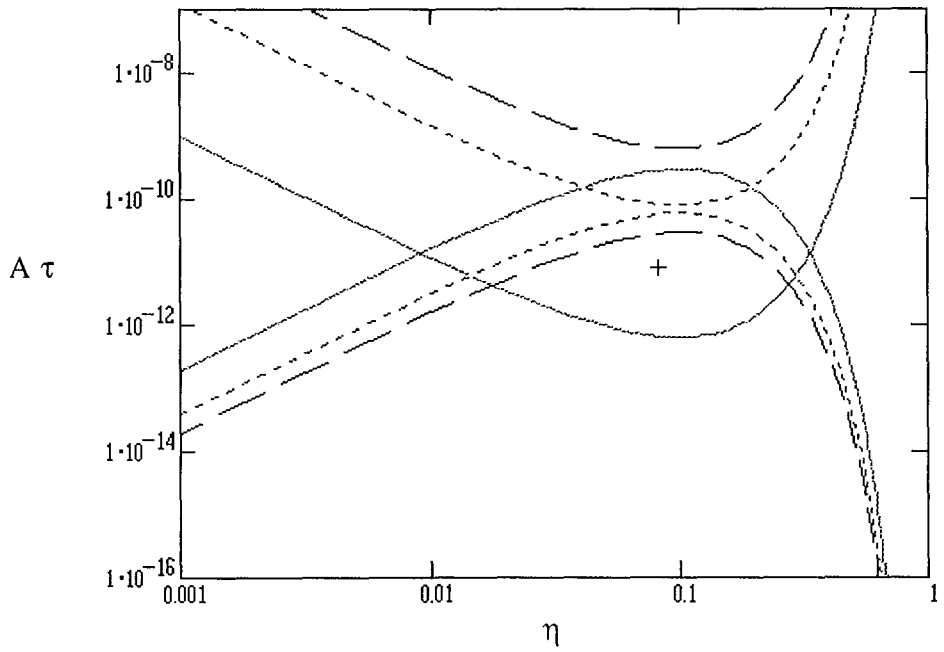

Fig. 8. The allowed region (marked with +) for 10 consecutive readings in η (hyperfine transition branching ratio) vs. Aτ (transition probability · data bit duration) space for a fractional increase in storage density of $N/k^2 = 2$ (limited by the solid lines), $N/k^2 = 10$ (limited by the dotted lines) and $N/k^2 = 20$ (limited by the dashed lines).

From figure 8 is it clear that to perform 10 consecutive readings from the storage sample with a signal to noise ratio of 10, with the limitations we so far have imposed on the storage medium, the fractional increase in storage density (N/k^2) must at least be smaller than 8.

For the cases shown in figure 8 it is only when the fractional increase in storage density (N/k^2) equals two, that we have the possibility of obtaining multiple reads. If we consider the case of a fractional increase in storage density of two, then the shrinking of allowed region for 1, 5, 25 and 45 consecutive reads is shown in figure 9. From figure 9 we obtain that when we have 45 or more consecutive reads, then the allowed region vanishes. This means that we have achieve a fundamental limit of the maximum number of reads, and this limit is 45 consecutive readings. This limit is set by the photon echo process itself and is therefore of great importance, but the number of reads are further restricted by the limits imposed by the material.

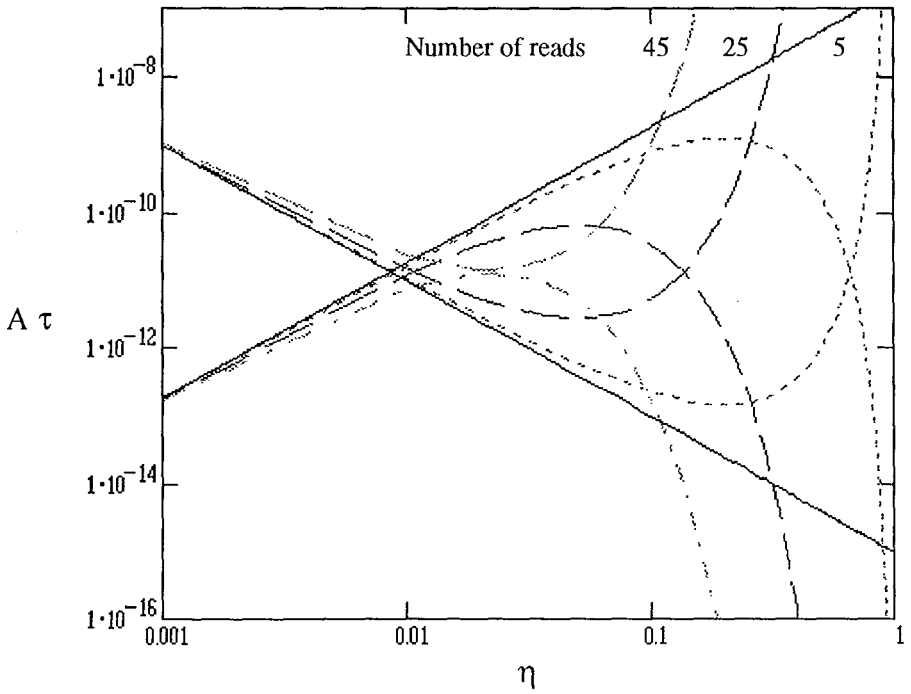

Fig. 9. The allowed region for a fractional increase in storage density (N/k^2) of 2, in η (hyperfine transition branching ratio) vs. $A\tau$ (transition probability · data bit duration) space for 5 reads (limited by the dotted lines),20 reads (limited by the dashed lines) and 45 reads (limited by the dash dotted lines).

It is worth noticing that in so called photon-gated storage[7] where upper state atoms after write and read pulses are forced into some reservoir state by a laser pulse of different wavelength, the available area in $(\eta, A\tau)$ space does not change with the number of reads. Instead the allowed value of $A\tau$ is given by figure 7 with $\eta = 1$. For any specific

storage/processing material there be further restrictions in the available (η,Aτ) space. This is described in the following sections.

3.5. Limitations set by the time- domain approach

The limits that we have imposed so far are that the data bit duration must be larger then or equal to the inhomogeneous relaxation time, equation (3.4), and the restriction that we only consider optical thin mediums, equation (3.7). These limits are sample independent and therefore the space between these two curves determines an intrinsic limit of the photon echo approach. However, this restrictions is not stringent enough, and we have to consider the following additional limits.

1. The laser intensity, I, should not be larger than the saturation intensity $I_{sat} = h\nu/(\sigma T_1)$, where T_1 is the upper state lifetime.

2. Thermal considerations limit I such that $I < I_{th} = 10^6$ W/m^2 (Ref. [10]).

3. The product of the electro-magnetic field at the focal point and the data-bit duration should be sufficient to rotate the Bloch vector the angle $\theta_D = \pi/(2N)$. Corresponding to transferring a fraction $1/4\cdot(\sin\theta_D)^2$ of the atoms to the excited state.

4. Eq. (3.7) is valid only for values of A sufficiently large that $n\sigma L = 0.3$ and must be extended to the case $n_{max}\sigma L \leq 0.3$.

These conditions put three new limits on τ. We now want to decide which values of the data-bit duration that are allowed. With the expression $\theta=(\mu E\tau)/$ for the pulse area can we rewrite condition 3 as a lower limit for the data-bit duration

$$\tau \geq \frac{\pi\hbar}{2N\mu E} \tag{3.12}$$

Furthermore, we know that the laser intensity is

$$I = \frac{1}{2} c\varepsilon_0 E^2 \tag{3.13}$$

and that we can express the transition dipole moment, μ, as[11]

$$\mu = \sqrt{\frac{3\varepsilon_0 h\lambda^3}{16\pi^3} A} \tag{3.14}$$

If we rearrange equation (3.13) and substitute this together with equation (3.14) in equation (3.12), we obtain

$$\tau > \pi\sqrt{\frac{\pi}{6}}\sqrt{\frac{hc}{\lambda^3}}\frac{1}{N}\frac{1}{\sqrt{IA}} \tag{3.15}$$

The assumption that we have a gaussian line width enable us to express the absorption cross section, σ, as

$$\sigma = \frac{T_{inh}\lambda^2}{4\sqrt{\frac{\pi}{\ln(2)}}}A \tag{3.16}$$

We can now with use of equation (3.16) express the saturation restriction on the laser intensity, condition 1, in terms of Einstein coefficient for the transition. These together with equation (3.15) give the final expression for the lower restriction of the data - bit duration:

$$\tau > \frac{\pi}{2}\frac{(\pi\ln(2))^{1/4}}{\sqrt{6}}\frac{\sqrt{T_1 T_{inh}}}{N} \tag{3.17}$$

From condition 2 we get that thermal considerations put an upper limit on the promoted laser intensity and this together with circumstance that the Bloch vector should be able to rotate an angle of $\theta_D = \pi/(2N)$ in the time τ, condition 3. This gives another lower limit of the data-bit duration.

$$\tau > \pi\sqrt{\frac{\pi}{6}}\sqrt{\frac{hc}{\lambda^3}}\frac{1}{N}\frac{1}{\sqrt{I_{th}A}} \tag{3.18}$$

To obtain this it is only to use condition 2 in equation (3.15). The actual lower limit is decided by which of these two restrictions that imposes the strongest condition on the process. To obtain an upper limit of the data-bit duration, we have to consider that we have an upper limit of the absorption in the sample, condition 4, For any specific material and transition, condition 4 can be fulfilled by rewriting equation (3.3) as

$$\tau < \frac{\pi^2}{64}\frac{3\eta_q}{\sqrt{\varepsilon}}n_{\max}^2\lambda^6\eta^2k^2\frac{T_{inh}^2}{\Pi}\frac{A}{(N/k^2)^2} \tag{3.19}$$

If we re-examine equation (3.7) then we realise that we can rewrite this as an upper limit for the data-bit duration. Further more is it clear that for small A is the limit imposed by equation (3.19) stronger than the limit of equation (3.7). To see how these limitations change allowed region we now consider a specific example.

3.6. Praseodymium

Consider the $^3H_4$ - $^1D_2$ transition in Pr^{3+}:$YAlO_3$ (see figure 5 in chapter 2.2 for energy level diagram). For this transition $A \cong 20\ s^{-1}$, $T_{inh} = 60$ ps, $T_1 = 180\ \mu s$ and $\eta = 0.06$ (see appendix A) [5]. To obtain the transition dependent restrictions on the data bit duration, τ, equations (3.18) and (3.19) are plotted vs the Einstein coefficient for the transition, A, in figure 10. The thermal limit, equation (3.18) (solid line), is independent of our choise of sample material, while equation (3.19) depends on the branching ratio, η and the inhomogeneous relaxation time. Equation (3.12) will give a limit below equation (3.13) in the region shown in figure 9 and will therefore not be drawn. The thermal limit is calculated assuming that the memory is continuously addressed. For data access frequencies, f_a, such that $f_a < 1/N\tau$ the thermal requirement for the storage material is relaxed and the solid curve is then adjusted downward.

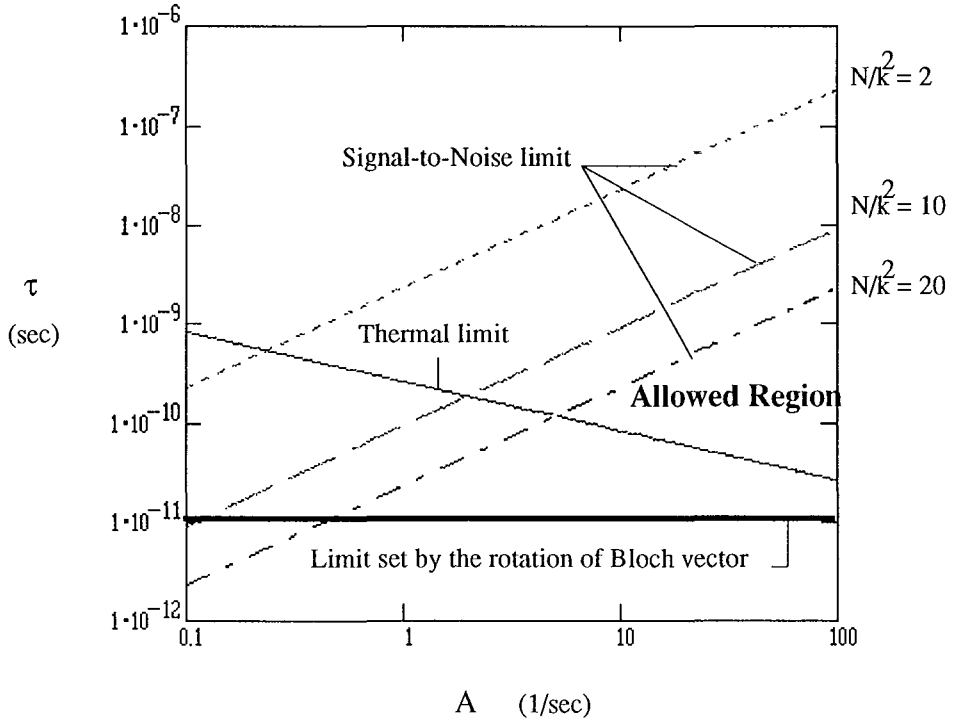

Fig. 10. Allowed data bit duration, τ, as a function of transition probability, A, for different values of N/k^2. Solid line, thermal limit. Dotted, dash dotted and dashed lines, signal - to - noise limit for $N/k^2 = 2, 10, 20$.

3.6.1.Processing Applications

When we use the storage medium for optical processing applications we are continuously addressing the medium and the thermal limit can not be relaxed. From figure 10 we get the allowed values of the data bit duration, τ, with respect to the limitations set by time-domain approach for a fractional increase in storage density (N/k^2) of 2, 10 and 20 , these are

N/k^2	Allowed τ	Corresponding $A\tau$
2	$5\cdot10^{-11} < \tau < 5\cdot10^{-8}$	$1\cdot10^{-9} < A\tau < 1\cdot10^{-6}$
10	$5\cdot10^{-11} < \tau < 2\cdot10^{-9}$	$1\cdot10^{-9} < A\tau < 4\cdot10^{-8}$
20	$5\cdot10^{-11} < \tau < 5\cdot10^{-10}$	$1\cdot10^{-9} < A\tau < 1\cdot10^{-8}$

For processing applications the branching ratio for the transition is equal to one. From figure 7 we see that the allowed values of the transition probability times data-bit duration, $A\cdot\tau$, are $10^{-15} < A\cdot\tau < 5\cdot10^{-7}$, $10^{-13} < A\cdot\tau < 10^{-7}$ and $10^{-12} < A\cdot\tau < 5\cdot10^{-8}$ for a fractional increase in storage density (N/k^2) of 2, 10 and 20. We have now imposed all the restrictions and are then able to decide the allowed parameter space when we use $Pr^{3+}:YAlO_3$ as an optical processor.

N/k^2	Allowed τ (s)	data processing rate	Occupying area for each kbyte
2	$5\cdot10^{-11} < \tau < 2\cdot10^{-8}$	500 MHz - 25 GHz	$4000\ \lambda^2$
10	$5\cdot10^{-11} < \tau < 5\cdot10^{-9}$	250 MHz - 25 GHz	$800\ \lambda^2$
20	$5\cdot10^{-11} < \tau < 5\cdot10^{-10}$	2,5 GHz - 25 GHz	$400\ \lambda^2$

6 References

[1] "Echoes in gaseous media: A generalized theroy of rephasing phenomena" T.W. Mossberg, R.Kachru and S.R.Hartman. Physical Review A**20** (1979) 1976

[2] "Generalized pertubation theory of coherent optical emission" M.Mitsunaga and R.G. Brewer, Physical Review A**32** (1985) 1605

[3] "Understanding optical echoes using Schrödinger's equation: Echoes excited by two optical pulses" A.V. Durrant, J.Manners and P.M. Clark, Eur. J.Phys. **10** (1989) 291.

[4] "SRI International Research Proposal No. PYC 85 - 097, Coherent Time - domain optical memory" R.Kachru and D.L. Huestis (1985).

[5] "Coherent transient and holeburning spectroscopy of rare earth ions in solids", R.M. Macfarlane and R.M. Shelby,109 in Spectroscopy of solids containing rare earth ions, Eds A.A. Kaplyanskii and R.M. Macfarlane, North - Holland 1987.

[6] "Photon Echoes", I.D. Abella, A Kurnit and S.R. Hartmann, Physical Review A**141** (1966) 391

[7] "Can single-photon process provide useful materials for frequency-domain optical storage?" W.E. Moerner and M.D. Levenson, Opt. Soc. Am. B(1985) 915

[8] "Resonance radiation and excited atoms", A.C.G. Mitchell and M.W. Zemansky, Cambridge university press, 1971.

[9] "Introduction to optical electronics", A. Yariv, Holt, Rinehart and Winston Inc, 1971

[10] "Fundamentals of Photonics", B.E.A. Saleh and M.C. Teich, John Wiley & Sons, 1991.

[11] "Einstein coefficients, cross sections, f values, dipole moments, and all that", R.C. Hillborn, Am. J. Phys. **50**,(1982) 982

[12] "Time - domain frequency - selective optical data storage", T.W. Mossberg, Optics Letters, **7** (1982) 77

[13] "248-bit optical data storage in Eu^{3+}:$YAlO_3$ by accumulated photon echoes", M. Mitsunaga and N. Uesugi, Optics Letters, **15** (1990) 195